Polymer Chemistry

ROYAL SOCIETY OF CHEMISTRY

PAPER

View Article Online
View Journal | View Issue

Cite this: *Polym. Chem.*, 2024, **15**, 4077

Mechanistic insights into *ortho*-blocked and *ortho*-free vitrimeric polybenzoxazines incorporating dynamic Schiff linkages for closed-loop recyclability†

Gaurav Rai and Leena Nebhani *

Vitrimers are an important breakthrough in the field of sustainable materials, particularly within the context of plastic waste management. These polymers can be designed with reversible linkages, which allows them to undergo bond exchange processes without compromising the integrity of the material. Hence, comprehending the correlation between the phenolic precursor used in benzoxazine monomer synthesis and subsequent vitrimeric properties obtained in polybenzoxazine networks can aid us in maximizing the potential of these reusable networks. This work presents an investigation using an *ortho*-blocked phenol (vanillin, 4-hydroxy-3-methoxybenzaldehyde) and an *ortho*-free phenol (4-hydroxybenzaldehyde) as aldehyde precursors, together with *p*-phenylenediamine as an amine precursor, facilitating the formation of dynamic imine networks. Before the formation of the imine network, phenolic groups were utilized for the formation of benzoxazines using stearylamine. The imine-containing benzoxazine monomers were subsequently subjected to further heating to induce polymerization. The inclusion of a methoxy group in a vanillin-based polybenzoxazine (PVBI) results in a reduced crosslinking density of 414 kJ mol^{-1}. In contrast, the polybenzoxazine (PHBI) synthesized using 4-hydroxybenzaldehyde exhibited a significantly higher crosslinking density (4842 kJ mol^{-1}). At a temperature of 25 °C, the storage modulus of PVBI was 115 ± 5 MPa, while the storage modulus of PHBI was 356 ± 5 MPa. The rheological properties demonstrate that a decrease in crosslinking density leads to a substantial reduction in relaxation time. This is because a lower crosslinking density allows higher chain mobility, facilitating exchange kinetics. Due to the topological reconfiguration of the structure induced by the exchange reaction between imine bonds, PVBI demonstrated remarkable malleability, having a stress relaxation time of less than 4 seconds, while PHBI had a stress relaxation time of 200 seconds at 120 °C. The activation energy determined from stress relaxation plots was 51 kJ mol^{-1} for PVBI and 68 kJ mol^{-1} for PHBI. The reprocessing studies conducted under hot-pressing showed that the mechanical properties, such as storage modulus and T_g, remained consistent even after three remolding cycles. Furthermore, incorporating imine bonds in the polybenzoxazine matrix facilitated a closed-loop recycling procedure where the material can be broken down into smaller fragments and then reassembled. After conducting recycling investigations, it was shown that 85% of the storage modulus was preserved in PVBI vitrimeric samples, indicating that these samples exhibit a significant degree of recyclability within a closed-loop system. The reprocessed and chemically recycled vitrimeric materials demonstrate significant preservation of thermal and mechanical properties.

Received 12th July 2024,
Accepted 3rd September 2024

DOI: 10.1039/d4py00776j

rsc.li/polymers

Department of Materials Science and Engineering, Indian Institute of Technology Delhi, Hauz Khas, New Delhi – 110016, India.
E-mail: Leena.Nebhani@mse.iitd.ac.in

†Electronic supplementary information (ESI) available: ^{1}H NMR of BASA, DSC comparison of BASA and PBASA, estimation of activation energy for benzoxazine curing using the Ozawa method, calculation of activation energy using stress relaxation studies, calculation of crosslink density, swelling studies in different solvents: (A) PVBI and (B) PHBI, swelling ratio in different solvents after 7 days, contact angle analysis performed on PVBI and PHBI, and FTIR of pristine and recycled PVBI. See DOI: https://doi.org/10.1039/d4py00776j

1. Introduction

Polybenzoxazines come under the umbrella of thermosetting polymers formed by the ring-opening polymerization of benzoxazine monomers derived from amines, formaldehyde and phenols. Polybenzoxazines are classified as phenolic resins because phenolic moieties make up the chemical structure of the polymer chains. The polymerization is initiated through thermal treatment of the monomer, triggering the benzoxazine

ring to open. This process does not require the use of harsh catalysts and does not result in the formation of byproducts. Polybenzoxazines are not prone to releasing harmful chemicals due to their chemical structure, and this, together with their self-catalyzed polymerization, makes them exciting material. Among their features are high thermal stability, near zero shrinkage upon polymerization, excellent dielectric, mechanical and thermal properties, and low flammability and water absorption, making them ideal material to replace conventional polymers. Their chemical design adaptability also provides a fantastic basis for using renewable feedstock. In the past, bio-based polybenzoxazines have been produced using cardanol, vanillin, and many other bio-phenols. Polybenzoxazines exhibit exciting features that render them suitable for diverse applications, including but not limited to excellent adhesives, polymer matrices for fibre-reinforced composites, and rigid PCBs (printed circuit boards). However, a prevalent issue faced by thermosetting resins is their limited recyclability and reprocessability, which poses a significant drawback.[1–3] Nevertheless, polybenzoxazines, like other thermosets, are not recyclable or reprocessable.

Thermosets cannot be recycled, reprocessed, or repaired because of their permanent three-dimensional crosslinked network resulting from irreversible chemical bonding. As a result, they cause significant environmental problems at the end of their lives. Many thermoplastics and thermosetting materials have recently been imbued with the "vitrimer" concept to make them malleable and reprocessable.[4,5] Covalent adaptable networks (CANs) are being utilized for this purpose. CANs have either a dissociative or associative mode of rearrangement.[6,7] In dissociative CANs, bond cleavage precedes bond formation (for example, Diels–Alder reaction). In contrast, in associative CANs (or vitrimers), linkages form an ever-evolving network where the formation of new bonds is preferred over breakage.[8,9] Consequently, the density of network crosslinks is maintained. Both cases result in crosslinked network structures, and due to inherent dynamic linkages, the networks can also reorganize themselves.[10] Growing interest in CANs has emerged at the macroscale level in polymer science and engineering, enabling the development of more sustainable thermosets.[11,12]

Polybenzoxazine networks have recently integrated different dynamic covalent linkages to enhance their reprocessability or self-healing properties. For instance, transesterification,[13–15] disulfide linkages, and boron ester linkages[16] were explored earlier to provide dynamic linkages in the polybenzoxazine networks. The use of imines as reversible links in dynamic materials has already been reported,[17,18] but polybenzoxazines containing imines are less explored. The fast exchange of imines can reduce both the reprocessability temperatures and cycle time used during hot-pressing compared to most other reversible bonds used in vitrimers. The imine exchange mechanism can be classified into three types: (i) imine exchange, (ii) amine exchange, and (iii) imine hydrolysis.[19–23] An excessive amount of amine might initiate the process of imine exchange through transamination.[24,25]

The use of bio-based precursors shows significant potential for the advancement of sustainable materials. As a result, the incorporation of vitrimer characteristics with biobased materials is seen as a novel and innovative merger.[26,27] The availability of biobased reactants and the extensive knowledge related to the formation of a Schiff linkage by condensation reactions between aldehydes and primary amines without any catalyst are favourable factors for reprocessing polybenzoxazines.[24–27] Furthermore, with this study, a better understanding can be developed on the effects of *ortho*-substitution with the use of two different phenols – vanillin (4-hydroxy-3-methoxybenzaldehyde) and 4-hydroxybenzaldehyde – on the mechanical properties and the dynamic behaviour in the case of vitrimeric polybenzoxazines.

Within the context of designing reusable, reprocessable, and recyclable high-temperature stable thermosets in mind, monomeric reactant synthesis was done utilizing biobased precursors like vanillin and stearylamine and precursors from petroleum feedstock such as 4-hydroxybenzaldehyde. The synthesis of novel benzoxazines with Schiff base linkages in benzoxazine-based thermosetting resins is described here. We envisioned that polybenzoxazines containing aromatic Schiff linkages would exhibit high reprocessability and decomposition temperature, given that aromatic polySchiffs possess outstanding thermal properties. The Schiff linkage-containing benzoxazine monomer was readily obtained by combining benzoxazine-containing aldehydes and diamines at room temperature. The vitrimers derived from polybenzoxazines contain rigid and highly polar imine linkages, which are reprocessable. With this approach, it is simple to modify the network structure and incorporate reversible imine linkages required for acquiring the final precursor for the polymerization step. The mechanical characteristics, stress relaxation, malleability, reprocessability, and weldability of vitrimeric polybenzoxazines were examined in depth in correlation with structural dependency. Based on our current understanding, this is the first work that dwells into the effect of phenol on the vitrimeric properties of polybenzoxazines containing dynamic imine linkages. The closed-loop recyclability was obtained using tetrahydrofuran (THF) as the solvent. By addressing the objectives outlined above, we hope to contribute to developing functionalized polybenzoxazines with improved mechanical properties and thermal stability, opening up new possibilities for their applications in diverse engineering fields.[28–31]

2. Experimental section

2.1 Materials

4-Hydroxybenzaldehyde was purchased from TCI Chemicals. Vanillin, *p*-phenylenediamine, sodium hydroxide, sodium sulphate, formalin, and paraformaldehyde were supplied by Loba Chemie. Bisphenol-A was purchased from Spectrochem. Stearylamine, ethanol, methanol, chloroform, hexane, THF,

acetone, and DMF were purchased from CDH Chemicals. Deuterated chloroform was purchased from Sigma Aldrich.

2.2 Synthesis procedure

2.2.1 Synthesis of a vanillin and stearylamine-based benzoxazine monomer containing a free aldehyde group (VB). The synthesis and characterization of vanillin and stearylamine-based benzoxazines with a free aldehyde group was performed using ethanol as a solvent. First, the reactant was taken in an optimized ratio of 1.1 : 0.8 : 2.0 for vanillin (4.4 mmol), stearylamine (3.2 mmol), and formalin (8.0 mmol), respectively. Stearylamine (3.2 mmol) was placed into a round-bottomed flask containing 16 mL of ethanol at room temperature. Dropwise addition of formalin was done with continuous stirring for 20 minutes. After this, vanillin (4.4 mmol) was introduced into the reaction flask, and the stirrer temperature was increased to 80 °C and refluxed for 7 hours. This was followed by gradual cooling to room temperature, resulting in a yellowish crystalline powder. The solid powder was purified through recrystallization using ethanol to yield a white solid containing the benzoxazine precursor possessing a free CHO-group. This was filtered and subsequently dried overnight in a vacuum oven at 45 °C.

^{1}H NMR ($CDCl_3$, 500 MHz): δ 0.87 (3H, t), 1.2–1.32 (27H, m), 1.51–1.64 (7H, m), 2.74 (2H, t), 3.93 (3H, s), 4.06 (2H, s), 5.05 (2H, s), 7.14 (Ar-1H, s), 7.28 (Ar-1H, s), 9.8 (1H, s).

^{13}C NMR ($CDCl_3$, 125 MHz): δ 10–40 (C_a and C_b), 49.69 (C_c), 51.50 (C_l), 56.02 (C_m), 83.95 (C_d), 107.87 (C_g), 120.50 (C_k), 124.89 (C_h), 128.94 (C_j), 148.35 (C_f), 149.70 (C_e), 190.88 (C_i).

2.2.2 Synthesis of a 4-hydroxybenzaldehyde and stearylamine-based benzoxazine monomer containing a free aldehyde group (HB). 4-Hydroxybenzaldehyde (4 mmol), stearylamine (3.2 mmol), and paraformaldehyde (8 mmol) were used in a 1.0 : 0.8 : 2.0 ratio and added to a 50 mL round-bottomed flask, which already contained 25 mL of chloroform, at room temperature, and then refluxed at 70 °C for 16 h and subsequently cooled to room temperature. Furthermore, the round bottom flask was added with 25 mL of chloroform and washed with water in a separating funnel. Afterward, the sample was dehydrated using magnesium sulfate, and the solvent was eliminated under reduced pressure, resulting in a powdered sample with an off-white tint.

^{1}H NMR ($CDCl_3$, 500 MHz): δ 0.87 (3H, t), 1.2–1.32 (33H, m), 1.51–1.64 (2H, m), 2.74 (2H, t), 4.0 (2H, s), 4.97 (2H, s), 6.89 (Ar-1H, d), 7.55 (Ar-1H, s), 7.67 (Ar-1H, d), 9.8 (1H, s).

^{13}C NMR ($CDCl_3$, 125 MHz): δ 10–40 (C_a and C_b), 49.87 (C_c), 51.43 (C_l), 83.47 (C_d), 117.02 (C_f), 120.59 (C_k), 129.47 (C_j), 129.77 (C_h), 130.30 (C_g), 160.30 (C_e), 191.03 (C_i).

2.2.3 Synthesis of a Schiff base (VBI) using a vanillin-based benzoxazine (VB) and phenylenediamine as the amine precursor. Two equivalents of VB (10 mmol) and one equivalent of phenylenediamine (5 mmol) were taken in a 150 mL round-bottomed flask. Nitrogen was purged for 30 minutes, and 50 mL methanol was added. In the presence of N_2, the temperature was raised to 45 °C and maintained for 3 h, resulting in the precipitation of a yellow-colored product. The yellow powder was obtained after several washings using methanol and drying it overnight in a vacuum oven at 45 °C.

^{1}H NMR ($CDCl_3$, 500 MHz): δ 0.87 (3H, t), 1.2–1.32 (27H, m), 1.51–1.64 (7H, m), 2.74 (2H, t), 3.93 (3H, s), 4.06 (2H, s), 5.05 (2H, s), 7.06 (Ar-1H, s), 7.24 (Ar-2H, s), 7.42 (Ar-1H, s), 8.36 (1H, s).

^{13}C NMR ($CDCl_3$, 125 MHz): δ 10–40 (C_a and C_b), 49.69 (C_c), 51.50 (C_l), 56.02 (C_m), 83.60 (C_d), 108.02 (C_g), 120.50 (C_k), 121.79 (C_j), 124.89 (C_o), 128.46 (C_h), 146.89 (C_n), 148.26 (C_f), 149.23 (C_e), 159.23 (C_i).

2.2.4 Synthesis of a Schiff base (HBI) using a 4-hydroxybenzladehyde-based benzoxazine (HB) and phenylenediamine as the amine moiety. The synthesis procedure was similar to the one used for the preparation of VBI, with the final precipitate being a yellow powder.

^{1}H NMR ($CDCl_3$, 500 MHz): δ 0.91 (3H, t), 1.2–1.32 (33H, m), 1.51–1.64 (2H, m), 2.74 (2H, t), 4.08 (2H, s), 4.97 (2H, s), 6.87 (Ar-1H, d), 7.28 (Ar-1H, s), 7.64 (Ar-2H, d), 8.41 (1H, s).

^{13}C NMR ($CDCl_3$, 125 MHz): δ 10–40 (C_a and C_b), 49.87 (C_c), 51.43 (C_l), 83.27 (C_d), 116.81 (C_f), 120.67 (C_n), 121.87 (C_K), 127.84 (C_j), 128.98 (C_g), 129.28 (C_h), 149.92 (C_m), 157.30 (C_e), 159.12 (C_i).

2.2.5 Synthesis of a control sample with the benzoxazine monomer having no imine bonds (BASA). Bisphenol-A (5 mmol), stearylamine (8 mmol), and formalin (40 mmol) were taken in a bisphenol-A : stearylamine : formalin ratio of 1 : 1.6 : 8.0, respectively. First, stearylamine was added to the reaction mixture containing 16 mL of ethanol at room temperature, followed by formalin addition and continuous stirring for 20 minutes. In addition, a precise quantity of bisphenol-A was introduced, followed by increasing the temperature to 80 °C for a duration of 7 hours. A white solid precipitated was obtained upon cooling, which was subsequently purified through recrystallization using ethanol.

^{1}H NMR ($CDCl_3$, 500 MHz): δ 0.9 (3H, t), 1.2–1.32 (24H, m), 1.51–1.64 (6H, m), 2.74 (2H, t), 3.95 (2H, s), 4.9 (2H, s), 6.68 (Ar-1H, d), 6.82 (Ar-1H, s), 6.96 (1H, d).

2.2.6 Synthesis of a vanillin and phenylenediamine Schiff base (VP). Vanillin (10 mmol) was added to a round-bottomed flask containing 15 mL of DCM. Subsequently, phenylenediamine (5 mmol) was gradually introduced into the reaction flask. The mixture was continuously stirred for 8 hours at a temperature of 45 °C. A yellow precipitate was obtained by cooling the reaction vessel, which was filtered, dried, and collected.

^{1}H NMR ($CDCl_3$, 500 MHz): δ 4.0 (3H, s), 6.0 (1H, s), 7.0 (1H, d), 7.25 (2H, d), 7.63 (1H, s), 8.40 (1H, s).

2.2.7 Imine exchange reaction between Schiff bases synthesized using vanillin and vanillin–stearylamine based benzoxazines (VPB). VP (5 mmol) and VBI (5 mmol) were added in 50 mL of chloroform at ambient temperature. The reaction was continuously refluxed at 70 °C for 7 hours, resulting in a dark solution that, when reduced under pressure, transformed into a red viscous substance labelled as VPB.

^{1}H NMR ($CDCl_3$, 500 MHz): δ 0.91 (3H, t), 1.2–1.32 (34H, m), 1.51–1.64 (2H, m), 2.74 (2H, t), 3.93 (6H, s), 4.08 (2H, s),

4.97 (2H, s), 6.7 (Ar-1H, d), 6.9 (Ar-1H, d), 7.0 (Ar-1H, s), 7.25 (4H, s), 7.44 (1H, s), 7.63 (1H, s), 8.37 (1H, s), 8.44 (1H, s).

2.2.8 Polymerization of benzoxazine monomers VBI and HBI. VBI was taken in small amounts in a boat-shaped Teflon mold. The powder was melted after heating for 30 minutes at 100 °C in a muffle furnace. The melted resin was transferred to molds of the preferred test configuration. The as-prepared samples were kept in a muffle furnace preheated at 100 °C for 30 minutes and cured at 170 °C for 4 h and 180 °C for 6 h. The resultant black compound was demolded after gradually cooling towards room temperature (PVBI).

The HBI sample was placed in a boat-shaped Teflon mold and then subjected to a temperature of 100 °C in a muffle furnace for a duration of 30 minutes. The powdered sample was melted and then transferred into the mold of the desired geometry for mechanical and rheological analysis. The samples were placed back inside the furnace for 30 minutes at 100 °C and then the temperature was slowly increased to 170 °C in the next 15 minutes at 5 °C min^{-1}. This was followed by isothermal curing for 4 h. After the samples underwent the curing process, they were cooled down to reach the ambient temperature and demolded to obtain samples for mechanical and rheological purposes (PHBI).

A control sample termed BASA was polymerized by curing the sample in a muffle furnace at 170 °C for 4 hours and 180 °C for 6 hours. This resulted in a transparent brown-colored compound (PBASA).

2.2.9 Reprocessing and reshaping of PVBI and PHBI resins. The polybenzoxazines were pulverized into a fine powder using a steel grinder and placed into DMA molds having a rectangular shape. Afterward, the molds were placed between the platens of a compression molding machine. The powder was compression molded for 10 minutes at 130 °C and 39 bar pressure using Labtech compression molding. Once the polybenzoxazine samples had cooled to ambient temperature, they were removed from the mold. The samples (PHBI and PVBI) were reshaped under the same conditions.

2.2.10. Solvent resistance. Tests were performed to evaluate the solvent resistance in DMF, ethanol, acetone, hexane, and water. The rectangular samples measuring 6 × 4 × 1.5 mm were submerged in several solvents simultaneously for a duration of one week at ambient temperature.

$$\text{Swelling ratio } (\%) = (m_s - m_i/m_i) \times 100$$

where m_s represents the swelled mass and m_i the initial mass.

2.2.11. Recyclability of the cured resins PVBI and PHBI. The cured polybenzoxazines were recycled with the help of THF by placing 1 g of sample (PVBI) in 30 mL of solvent. The solution underwent a color change to black when it was heated to a temperature of 60 °C for 2 hours and subsequently cooled down to ambient temperature. Following a duration of 6 hours, the sample was placed in an air oven set at a temperature of 100 °C to facilitate the evaporation of the solvents, giving a black powder in the end. The black powdered material was hot-pressed at 130 °C for 10 minutes and 39 bar pressure to obtain the recycled PVBI. PHBI was tested for recycling under similar conditions.

3. Characterization

The FT-IR spectra in the 400–4000 cm^{-1} region were recorded with a resolution of 4 cm^{-1} using a Thermo Fisher Scientific Nicolet IR 200 spectrometer equipped with an attenuated total reflection (ATR) accessory. The samples were analyzed using a Bruker AC 500 MHz nuclear magnetic resonance (NMR) spectrometer to acquire the ^{1}H NMR and ^{13}C NMR spectra. The spectra were recorded using deuterated chloroform ($CDCl_3$), with tetramethylsilane (TMS) as the internal standard. The curing profiles of the samples were obtained using a TA Instruments Q 2000 differential scanning calorimeter (DSC). The samples, weighing 5 ± 1 mg, were placed in aluminum pans and subjected to heating under a nitrogen atmosphere. The temperature was increased from 0 to 400 °C at a rate of 10 °C per minute to conduct DSC scanning. Once the sample was placed, it took one minute for thermal equilibrium to be achieved. The exothermic reaction was considered complete when the signal stabilized at the baseline. The rheological behavior of the resin was investigated using an Anton Paar Rheometer MCR-702. The thermal behavior between 30 and 800 °C was investigated under a nitrogen atmosphere with an ideal flow rate of 50 mL min^{-1} by means of a thermogravimetric analyzer (TA Instruments Q500). Each experiment made use of a 5 ± 0.5 mg sample mass and a 20 °C min^{-1} heating rate. A TA Instruments Q800 DMA was used to conduct dynamic mechanical analysis (DMA) on rectangular specimens measuring approximately 20 × 8 × 1.8 mm. The specimens were subjected to a controlled heating process, between 0 and 140 °C, at a constant inflation rate of 5 °C per minute. The samples were subjected to a strain amplitude of about 1.0% at a frequency of 1 Hz. The glass transition temperature (T_g) was determined by examining the peak of the tangent delta (tan δ). A drop shape analyser (DSA100E) was employed to measure the contact angle using ultra-pure water at ambient temperature. Specimens for measurements were prepared by putting the cured resin onto a glass slide. The thickness of the polybenzoxazine coating was sufficient to impede any interference caused by the hydrophilic glass during the measurements. The planar surfaces of the thermosets were utilized to measure the contact angle.

4. Results and discussion

4.1 Synthesis of two Schiff base containing benzoxazine monomers

Two different synthetic routes were followed for the formation of benzoxazines containing a free aldehydic group, *i.e.* vanillin based benzoxazine (VB) and hydroxybenzaldehyde based benzoxazine (HB), as shown in Scheme 1. In the case of VB, the synthesis procedure involves ethanol as the solvent and vanil-

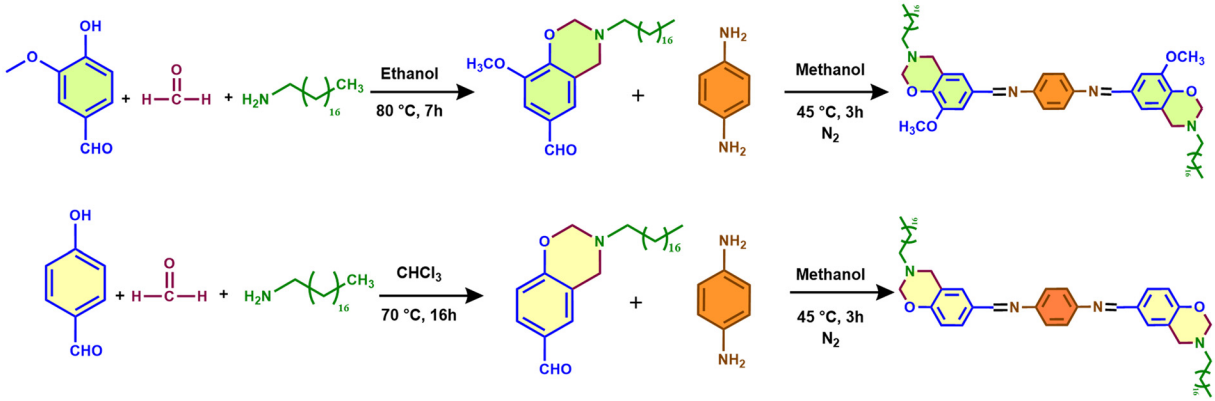

Scheme 1 Synthesis routes for obtaining two different Schiff base functionalized benzoxazine monomers: (A) VBI and (B) HBI.

lin as the phenolic precursor. A white powder that was obtained after the crystallization process was dissolved in $CDCl_3$, and the ^1H NMR analysis showed peaks at approximately 5.0 and 4.0 ppm (Fig. 1(A)), indicating the presence of oxazine (–O–CH_2–N–) and Mannich (–C–CH_2–N–) linkages. In addition, the –O–CH_3 group linked to the benzene ring of vanillin exhibits a singlet at 3.9 ppm. The aldehydic protons at the *para*-position were confirmed with the help of the singlet appearing at 9.8 ppm.

The synthesis of HB was performed in chloroform under reflux conditions with 4-hydroxybenzaldehyde as the phenolic precursor. All the reactants were added simultaneously into a round-bottomed flask. The obtained product was analyzed using ^1H NMR spectroscopy (Fig. 1(E)). The spectroscopy showed distinct benzoxazine peaks at 5.0 ppm, indicating the presence of the oxazine (–O–CH_2–N–) linkage, and peaks at 4.0 ppm, indicating the presence of the Mannich linkage (–C–CH_2–N–). The peak identified at 9.8 ppm confirms the presence of –CHO, giving us a benzoxazine monomer (HB) containing a free aldehydic moiety. The ^{13}C NMR analysis of both VB (Fig. 1(C)) and HB (Fig. 1(G)) provides the confirmation of the presence of oxazine carbon at 83 ppm and Mannich carbon at 52 ppm. The carbon atom in the aldehyde functional group of VB and HB is located at around 190 ppm.

The formation of benzoxazine monomers containing Schiff linkages (VBI and HBI) was carried out using identical chemical routes (Scheme 1). Under an inert atmosphere, methanol was used as the solvent in a 2 : 1 reaction between VB/HB and *p*-phenylenediamine at ambient temperature. The yellow precipitate obtained was filtered and characterized using ^1H NMR and FTIR spectroscopy. The imine bond (–H–C=N–) in ^1H NMR appears as a singlet at 8.36 ppm for VBI (Fig. 1(B)) and 8.41 ppm for HBI (Fig. 1(F)), signifying a single proton, whereas the aldehyde peak near 9.8 ppm was not observed, which confirms complete conversion.[32] The integration of the entire ^1H NMR spectra gave us the exact number of protons confirming a benzoxazine containing a Schiff base. This was further supported by ^{13}C NMR spectroscopy (Fig. 1(D) and (H)), where the peak around 190 ppm for –CHO is replaced by a peak at 160 ppm corresponding to the imine bond.

4.2. Model compound study for the exchange reaction between dynamic imine bonds

A small molecule investigation was carried out to learn more about the exchange behavior shown by imine bonds. A critical factor in forming vitrimers is the consistency of exchange reactions. Imine chemistry, commonly called Schiff base chemistry, uses the properties of a typical reversible covalent interaction and is widely used in synthesizing recyclable materials. To support the idea that imine bonds are dynamic, a specific type of reaction was done to verify this hypothesis. A small molecule model was utilized to investigate the dynamic exchange reaction features of imine bonds with the help of ^1H NMR spectroscopy. A detailed synthesis process for the model compounds (Fig. 2(A)) used in the study is provided in the Experimental section. Two molecules, VP and VBI, with symmetrical structures were selected for this study. After that, a mixture of VP and VBI was refluxed for seven hours at 70 °C to facilitate a dynamic reversible exchange reaction. This reaction will lead to the formation of "VBP" provided that the predicted dynamic exchange reaction occurs. The reaction was slowly cooled to room temperature. The chloroform was evaporated using pressure, resulting in the formation of a thick crimson viscous liquid. This viscous liquid was then subjected to analysis using ^1H NMR spectroscopy. The ^1H NMR spectra of VP (Fig. 2(B)) and VPB (Fig. 2(C)) are shown for comparative analysis. The ^1H NMR spectra shown in Fig. 2(C) revealed two different singlets at 8.4 and 8.3 ppm related to two distinct imine linkages. These two different imine peaks are only possible when the exchange has occurred at one end of the imine, *i.e.*, when one Schiff linkage from VP is exchanged with a Schiff linkage from VBI, resulting in VBP containing two distinct Schiff linkages. This was further supported by six protons of –OCH_3– detected at 3.9 ppm, implying two methoxy groups from two different units of vanillin used in benzoxazine formation (VBI) and vanillin used in Schiff base formation (VP). Multiple signals were seen in the aromatic area and attributed to the aromatic protons in VBP. The spectra confirmed that the exchange process between two different Schiff bases has occurred at high temperatures. Thus, imine bonds can be exploited to create vitrimer-like materials.

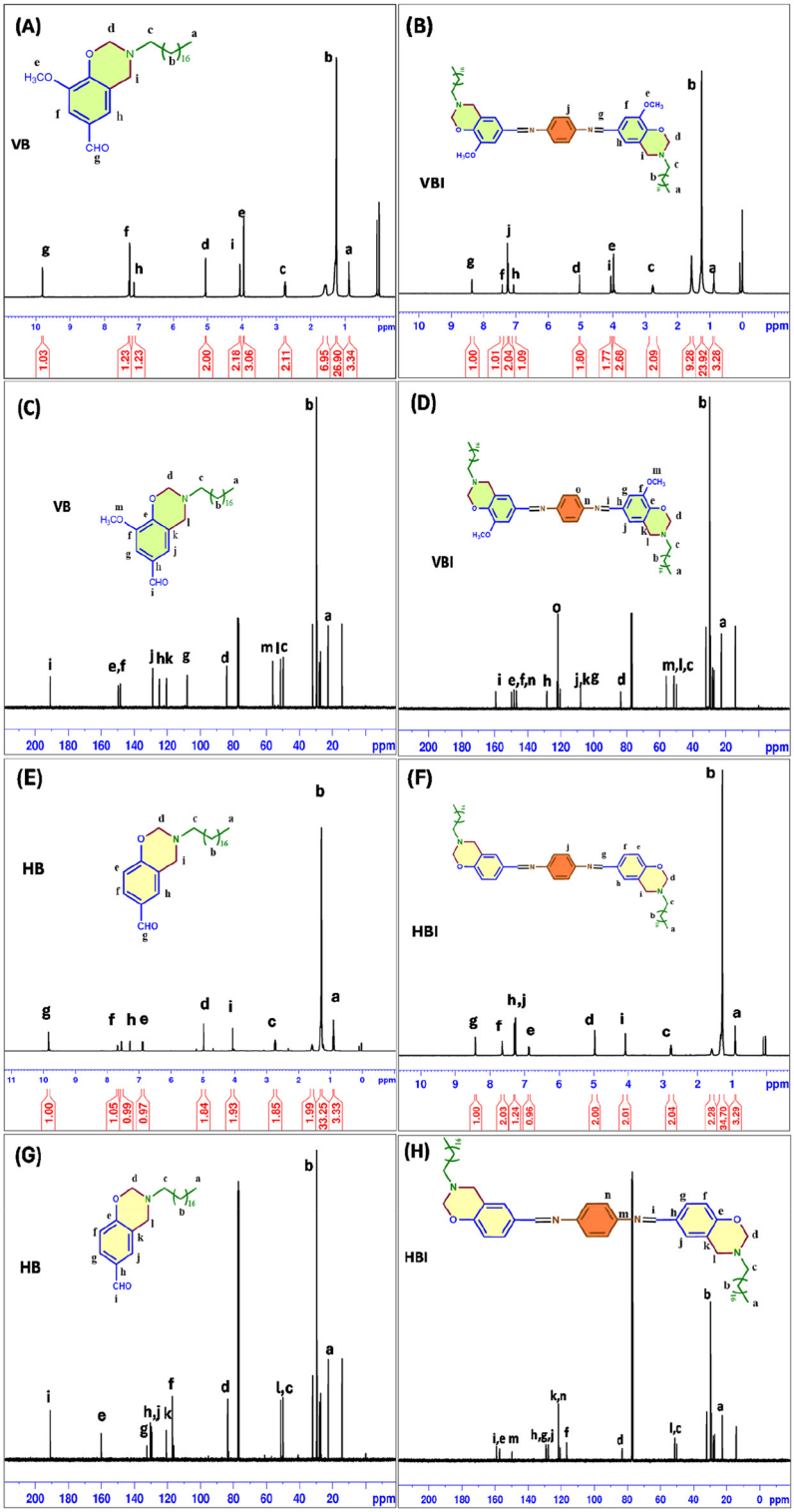

Fig. 1 (A) ^{1}H NMR spectrum of VB, (B) ^{1}H NMR spectrum of VBI, (C) ^{13}C NMR spectrum of VB, (D) ^{13}C NMR spectrum of VBI, (E) ^{1}H NMR spectrum of HB, (F) ^{1}H NMR spectrum of HBI, (G) ^{13}C NMR spectrum of HB, and (H) ^{13}C NMR spectrum of HBI.

4.3 Curing kinetics and curing behaviour

Using non-isothermal differential scanning calorimetry (DSC) at heating rates of 5, 10, 15, and 20 °C per minute, the curing kinetics of VBI and HBI were investigated to determine an ideal curing profile. According to Fig. 3, the peak polymerization temperature (T_p) for both VBI and HBI shifted towards higher values when the heating rate (β) was increased. The

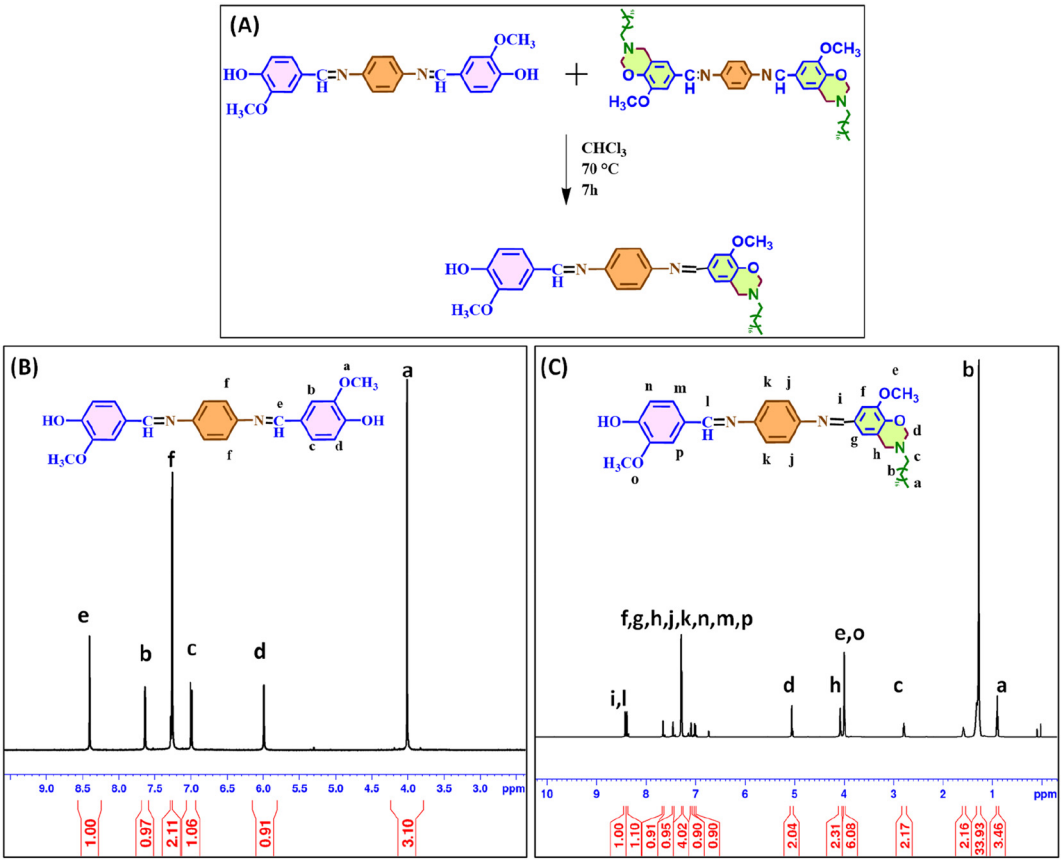

Fig. 2 (A) Small molecule study performed by dissolving VP and VBI together in chloroform, (B) ^{1}H NMR spectrum of VP and (C) ^{1}H NMR spectrum of VPB.

Ozawa equation was used to find the activation energy (E_a) of the curing reaction (1).

$$\ln(\beta) = -1.052\frac{E_a}{RT_p} + C \quad (1)$$

where R is the gas constant and C is a constant.

The Ozawa approach resulted in activation energy (E_a) values of 98 kJ mol^{-1} for HBI and 122 kJ mol^{-1} for VBI (Table S1†), as shown in Fig. 3. We observed that HBI had lower E_a values compared to VBI, suggesting that the presence of the methoxy group causes steric hindrance, hence delaying the polymerization reaction, as illustrated in plausible curing mechanisms shown in Fig. 4.

The polymerization mechanism in *ortho*-blocked VBI is illustrated in Fig. 4(A) and (B). Two distinct pathways comprise the plausible polymerization mechanism. First, a *meta*-attack on the iminium carbon of the ring-opened benzoxazine monomer may occur, in which case the polymer chain will continue to grow at the *meta*-position of vanillin in VBI. Secondly, the iminium carbon can also be attacked by the hydroxy group of the vanillin as a result of the delayed reactivity of the *meta*-attack. The curing mechanism for the *ortho*-free benzoxazine monomer (HBI) is illustrated in Fig. 4(C). The *ortho*-site is the most efficient at attacking the iminium carbon due to its high electron density. Consequently, polymerization occurs at a rapid pace in comparison with VBI.[33–35] Based on the activation energy for the polymerization of benzoxazine monomers obtained by DSC and the plausible mechanism, VBI was heated in a muffle furnace at 100 °C for 30 minutes, followed by 4 hours at 170 °C and 6 hours at 180 °C. HBI, on the other hand, was heated to 100 °C for 30 minutes and 4 hours at 170 °C.

The DSC plot (Fig. 5(A) and (B)) shows a comparison between polybenzoxazines (PVBI and PHBI) and benzoxazine monomers (VBI and HBI) revealing no exothermic peaks associated with the oxazine moiety in the polybenzoxazines. Therefore, the oxazine linkage in the Schiff-containing benzoxazine monomer underwent ring opening, which facilitated the complete polymerization with the end product being polybenzoxazines with dynamic imine linkages. Due to the variable curing reactivity of the phenols involved in monomer development, on examining the curing behavior of two benzoxazine monomers, VBI (Fig. 5(A)) and HBI (Fig. 5(B)) revealed clear exothermic peaks within the temperature range of 230 to 250 °C, corresponding to thermally induced cationic ROP of the benzoxazine monomer. When comparing VBI and HBI, it is observed that HBI has a greater curing enthalpy (ΔH) of 92 J g^{-1}, while VBI has a lower

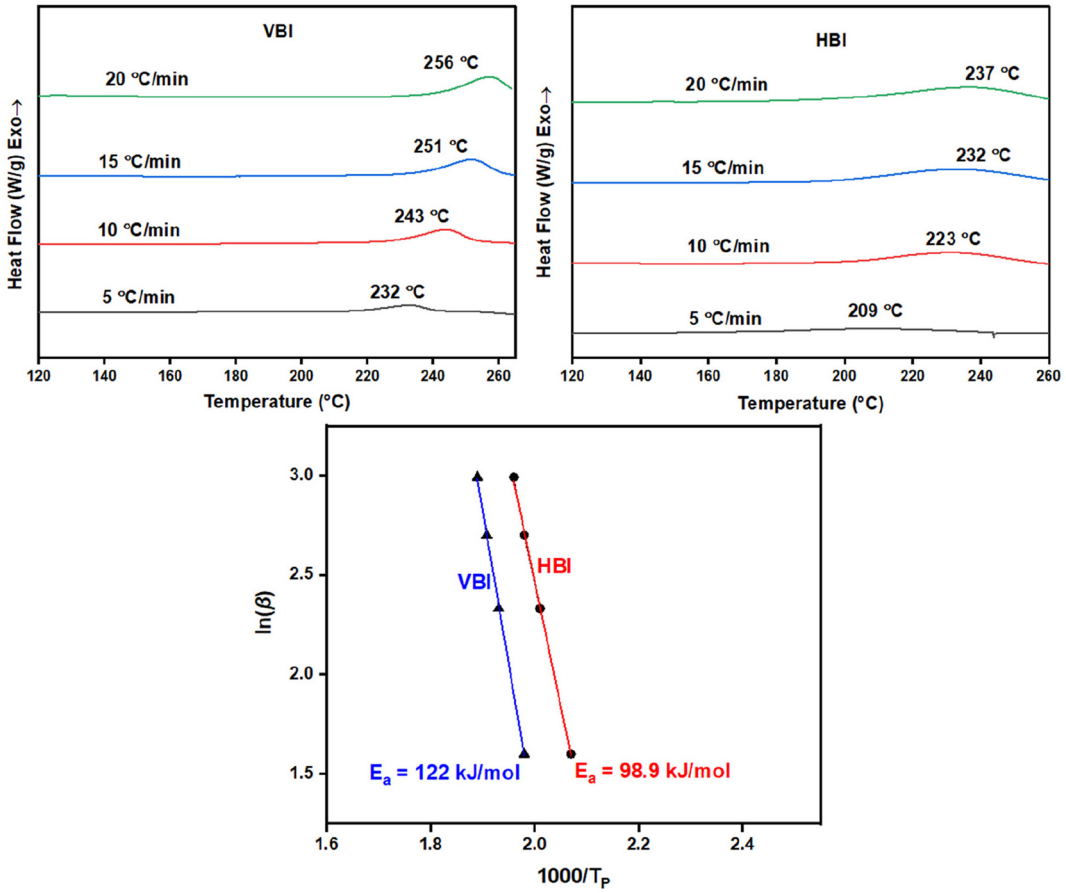

Fig. 3 Non-isothermal differential scanning calorimetry results of VBI and HBI with the kinetic parameters of VBI and HBI calculated by the Ozawa method.

value of 40.81 J g^{-1}. This difference in ΔH values signifies that the curing reactivity of HBI surpasses that of VBI. Unlike VBI, HBI demonstrates increased curing reactivity during the early phases of the curing process.

The FTIR spectra of VB shown in Fig. 5(E) contain bands for aldehydic C═O stretching vibration (1663 cm^{-1}). The –CH_2– group in the oxazine linkage and the alkyl chain derived from stearylamine exhibit bands corresponding to asymmetric and symmetric stretching vibrations at wavenumbers of 2920–2853 cm^{-1}. The –C–O–C– bond exhibits asymmetric stretching, with peak frequencies observed at 1222 cm^{-1}, and the –C–N–C– asymmetric stretching appears at 1140 cm^{-1}.

The FTIR analysis of HB (Fig. 5(F)) shows a band at 1665 cm^{-1}, corresponding to the stretching vibrations of the aldehydic –C═O group. Additionally, the asymmetric vibration band of the (–C–O–C–) group, which corresponds to the oxazine linkage, emerges at 1230 cm^{-1} and the (–C–N–C–) asymmetric stretching at 1142 cm^{-1}, referencing the Mannich base, can be seen.

FTIR spectroscopy was used to compare the spectra of VB and HB (Fig. 5(E) and (F)) with VBI and HBI, respectively. In the spectra, the band corresponding to the aldehyde group (–C═O stretching vibration) at 1663 cm^{-1} was no longer present, while new bands associated with the imine group (–C═N stretching vibration) appeared at 1635 cm^{-1}, confirming the formation of imine bonds, whereas the C–H stretching vibration (2850–2950 cm^{-1}) and –C–N–C– stretching vibration around 1140 cm^{-1} remain unaffected during the conversion from aldehyde to imine.

The FTIR spectra depicted in Fig. 5(E) and (F) demonstrate the lack of an asymmetric stretching vibration of oxazine (–C–O–C–) in both PVBI and PHBI, whereas –C–N–C– is present in all the spectra. This validates that the process of curing has been accomplished successfully.[36,37] The polymerization mechanism ensures that dynamic linkages will be retained during the curing process, allowing the formation of three-dimensional crosslinked networks through the imine bonds that connect two polymer chains.

4.4 Thermal and mechanical properties of benzoxazines containing Schiff linkages

The powdered monomer samples were polymerized at different temperatures using the previously specified curing profile, resulting in a solid homogeneous product with no voids. Thermogravimetric analysis (TGA) was performed on

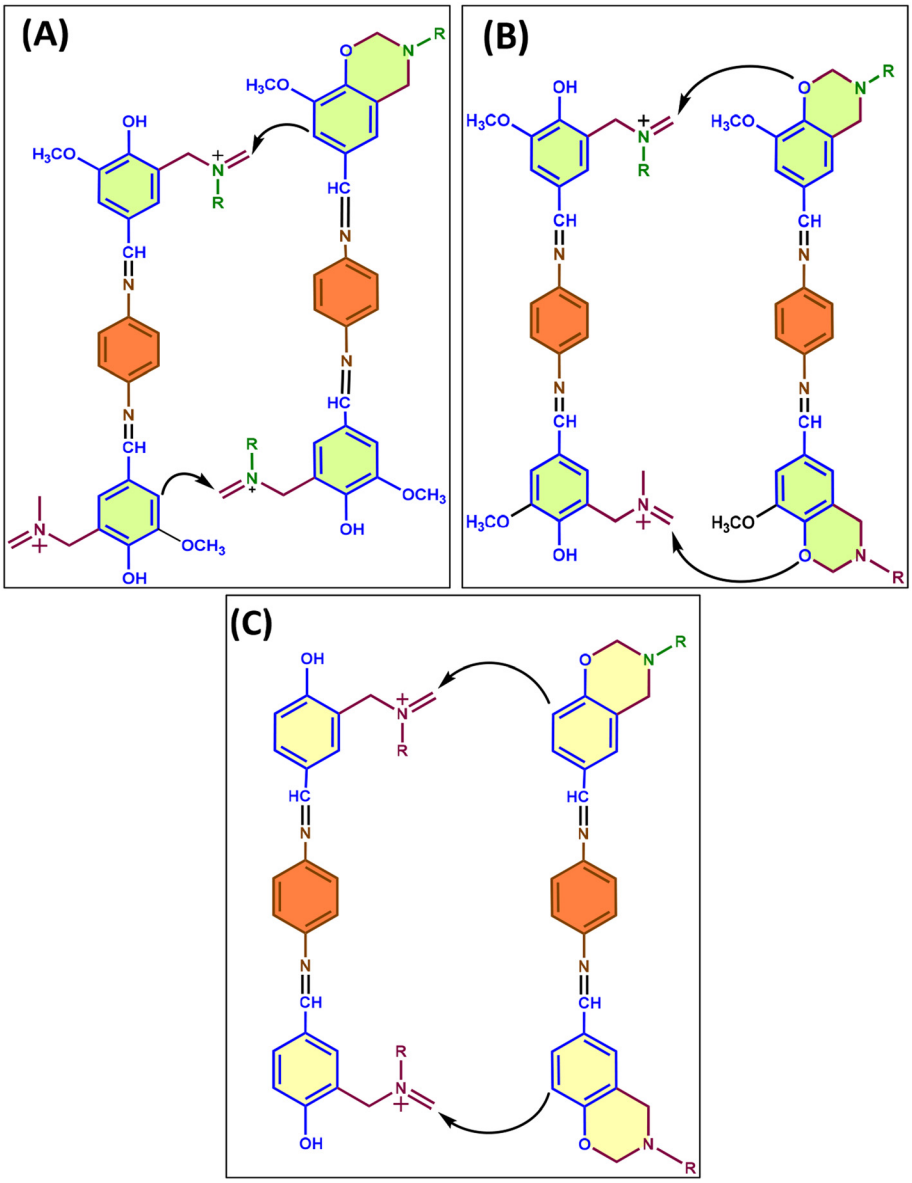

Fig. 4 (A) Plausible mechanisms of polymerization in an *ortho*-blocked polybenzoxazine *via* a *meta*-attack, (B) Plausible mechanisms of polymerization in an *ortho*-blocked polybenzoxazine *via* a hydroxy attack and (C) Plausible mechanisms of polymerization in an *ortho*-free polybenzoxazine *via* an *ortho*-attack.

the samples as depicted in Fig. 5(C) and (D), clearly demonstrating that the crosslinked 3D network provides good thermal stability as indicated by the 5% degradation temperature, or $T_{5\%}$. The $T_{5\%}$ for PVBI and PHBI is 269 °C (Fig. 5(C)) and 285 °C (Fig. 5(D)), respectively. The increased stability of PHBI is attributed to the free *ortho*-position in 4-hydroxybenzaldehyde, which provides no steric hindrance for the *ortho*-attack on the iminium carbon. The –OCH_3– group in vanillin restricts the reaction with the iminium carbon, thereby delaying this step and enabling the *meta*-attack to progress, as demonstrated by the mechanism. Although the *meta*-site is available for polymerization in HBI monomers, the preferred site for bond formation is the *ortho*-position.

The theoretical molecular crosslink weight (M_c) represents the theoretical molecular weight between the crosslinks leading to an idea of predicting the overall stability of the polymer. The M_c of both the polybenzoxazines was calculated using the following equation, where n is the number of moles of the compound and M is the molar mass of the compound:

$$M_c = \frac{n_{CHO} \times M_{CHO} + n_{diamine} \times M_{diamine} - 2n_{diamine} \times M_{H_2O}}{n_{diamine}} \quad (2)$$

A higher M_c means a high molecular weight between crosslinks, indicating the presence of long chains in the

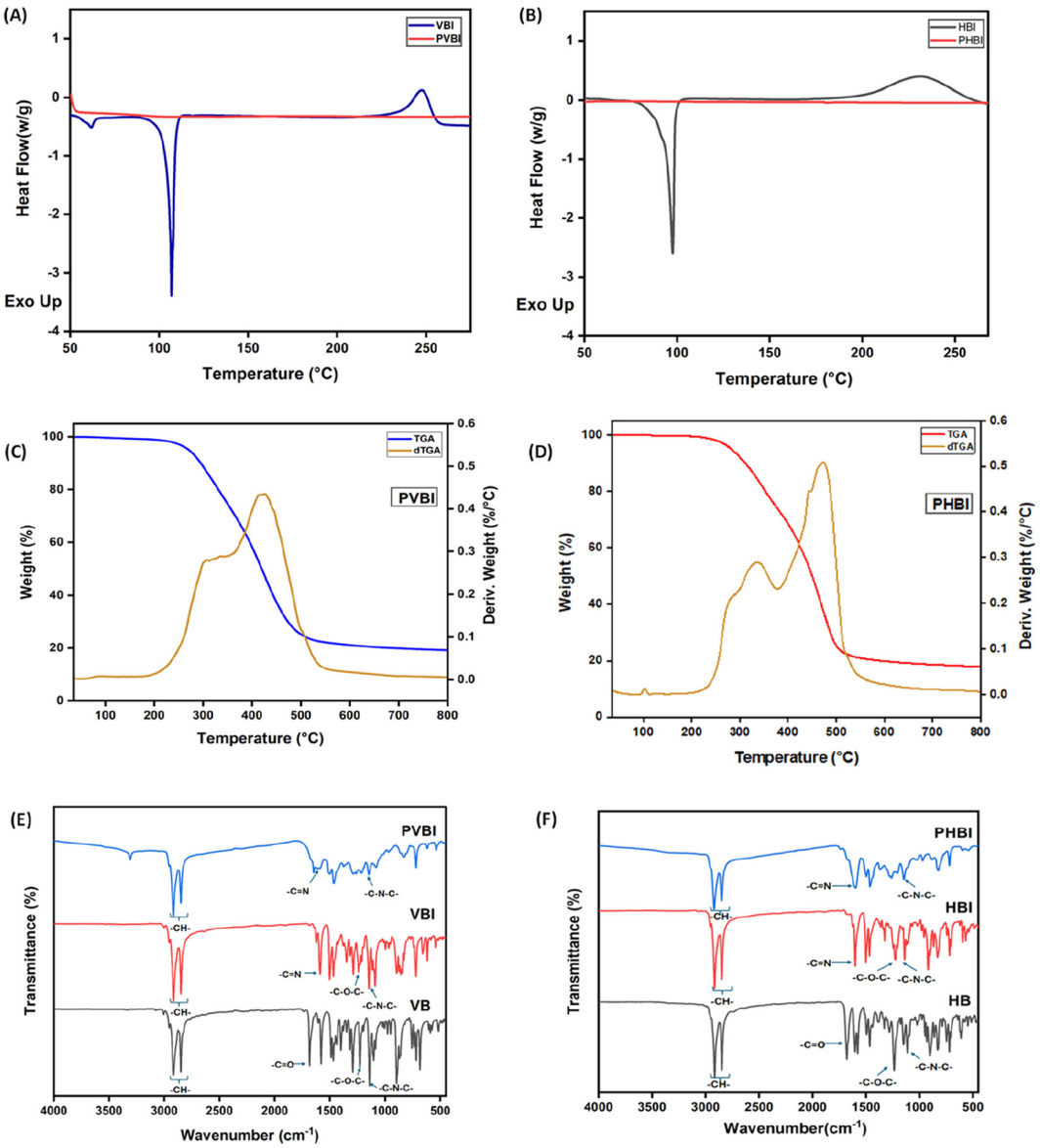

Fig. 5 (A) DSC comparison of VBI and PVBI, (B) DSC comparison of HBI and PHBI, (C) TGA and dTGA of PVBI, (D) TGA and dTGA of PHBI, (E) FTIR comparison of PVBI with VBI and VB, and (F) FTIR comparison of PHBI with HBI and HB.

polymeric network. In contrast, a lower M_c means multiple crosslinks due to the short chain length. Therefore, a higher M_c means lower stability. The determination of M_c was done using eqn (2),[38] which is 481 g mol^{-1} for PVBI and 451 g mol^{-1} for PHBI. A higher molecular weight between crosslinks means a lower crosslink density. Experimentally, this finding is corroborated by DMA analysis by calculating the crosslink density (ν) of the polybenzoxazines using rubber elasticity eqn (3), where E' represents the plateau storage modulus from the elastic region of the DMA analysis, R is the ideal gas constant and T is the temperature at which E' is taken. The DMA result reveals a crosslink density that is ten times higher in the case of PHBI (4842 mol m^{-3}) compared to PVBI (414 mol m^{-3}), as shown in S3.†[39]

$$\nu = \frac{E'}{3RT} \quad (3)$$

When comparing the properties of PHBI and PVBI, the findings of DMA indicate that PHBI possesses a rigid polymeric structure, whereas PVBI exhibits a weak nature. Throughout the investigation, the storage modulus values for PHBI consistently outperformed those of PVBI over the whole temperature range, as shown in Fig. 6. This is due to the fact that longer polymeric chains are generated in PHBI because *ortho*-positions are readily available in every monomeric unit

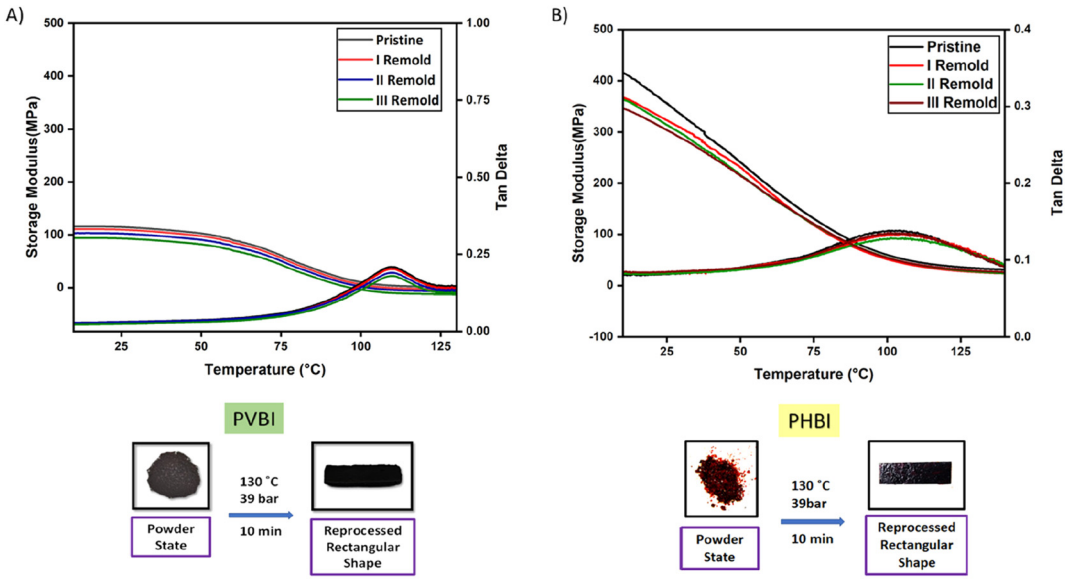

Fig. 6 (A) Storage modulus and tan δ *vs.* temperature plots in PVBI along with reprocessing images and conditions and (B) Storage modulus and tan δ *vs.* temperature plots in PHBI along with reprocessing parameters used in hot-pressing.

for bond formation with iminium carbon. Vanillin, on the other hand, contains a methoxy group that interferes with this action. As a result, the *meta*-attack on the iminium carbon proceeds slowly.

The tan δ has a single peak in both polybenzoxazine networks, indicating a homogeneous ROP of the benzoxazine network in *ortho*-blocked and *ortho*-free polybenzoxazines. The presence of a stable rubbery plateau suggests that the crosslinking density is retained at elevated temperatures.[40,41] The tan δ peaks differ between PHBI and PVBI, with the former being broad and the latter being sharp. The tan δ peak indicates the occurrence of a molecular relaxation process in the polymer. A broad peak shows various relaxation processes at different temperatures, indicating the presence of multiple polymer segments containing dynamic bonds within the material.[42] This implies a bigger range of temperatures where the polymer shows viscoelastic behavior. Because there are many molecular crosslinks in PHBI, various polymer segments may have varying relaxation and glass transition temperatures, broadening the tan δ curve. A steep tan δ peak implies high energy dissipation capability, implying that the polymer is more viscoelastic. This is indicated by the malleable nature of PVBI at higher temperature.

Adding imine bonds would be anticipated to enable PVBI and PHBI to be reprocessable, much like the reported literature on imine reversible networks. The polybenzoxazine powder can be turned into a solid resin form after hot-pressing treatment. This property was verified by finely powdering PVBI and PHBI and pressing them in a steel mold for 10 minutes at 130 °C and 39 bar pressure, respectively. The results from the DMA analysis show that the storage modulus is unaltered despite three rounds of reprocessing and only marginally lower with additional reprocessing cycles. This could result from the polybenzoxazine resin's thermal aging and defect buildup caused by hot-pressing treatment.

The thermomechanical properties of both virgin and reprocessed PVBI and PHBI were examined by DMA. The relevant data are summarised in Fig. 6, which also displays the storage modulus and tan δ as a function of temperature. At 25 °C, the glassy state storage modulus of virgin PVBI is 115 MPa, as shown in Fig. 6(A), while that of PHBI is 356 MPa, as depicted in Fig. 6(B). The peak temperature of tan δ determines the glass-transition temperature (T_g). The glass transition temperature (T_g) for virgin PVBI is 107 °C, while for virgin PHBI it is 110 °C. Fig. 6 demonstrates that the storage modulus of PHBI is higher than that of PVBI, even when considering reprocessed samples. This further supports the increased curing degree of PHBI. It is essential to mention that the retention of T_g is greater than 95% for mechanically reprocessed polybenzoxazine resins exhibiting the effect of the associative imine linkage in retaining the crosslink density. The strong retention of thermo-mechanical properties can be attributed to the crosslink networks' continued integrity even after many reprocessing cycles.

4.5 Solvent resistance and surface properties

Imine chemistry is distinguished by the presence of reversible covalent interactions, such as hydrolysis, imine–imine exchange, and amine–imine exchange (transamination), that occur in organic solvents.[43] As such, it is essential to evaluate the solvent resistance of PVBI and PHBI. Fig. S3† displays the pictures of polybenzoxazines that have been left in various solvents for one week at room temperature, including THF, DMSO, DMF, EtOH, water, and hexane. According to Table S3,† in different solvents,[44,45] PHBI has a excellent solvent resistance than PVBI. This suggests that the highly

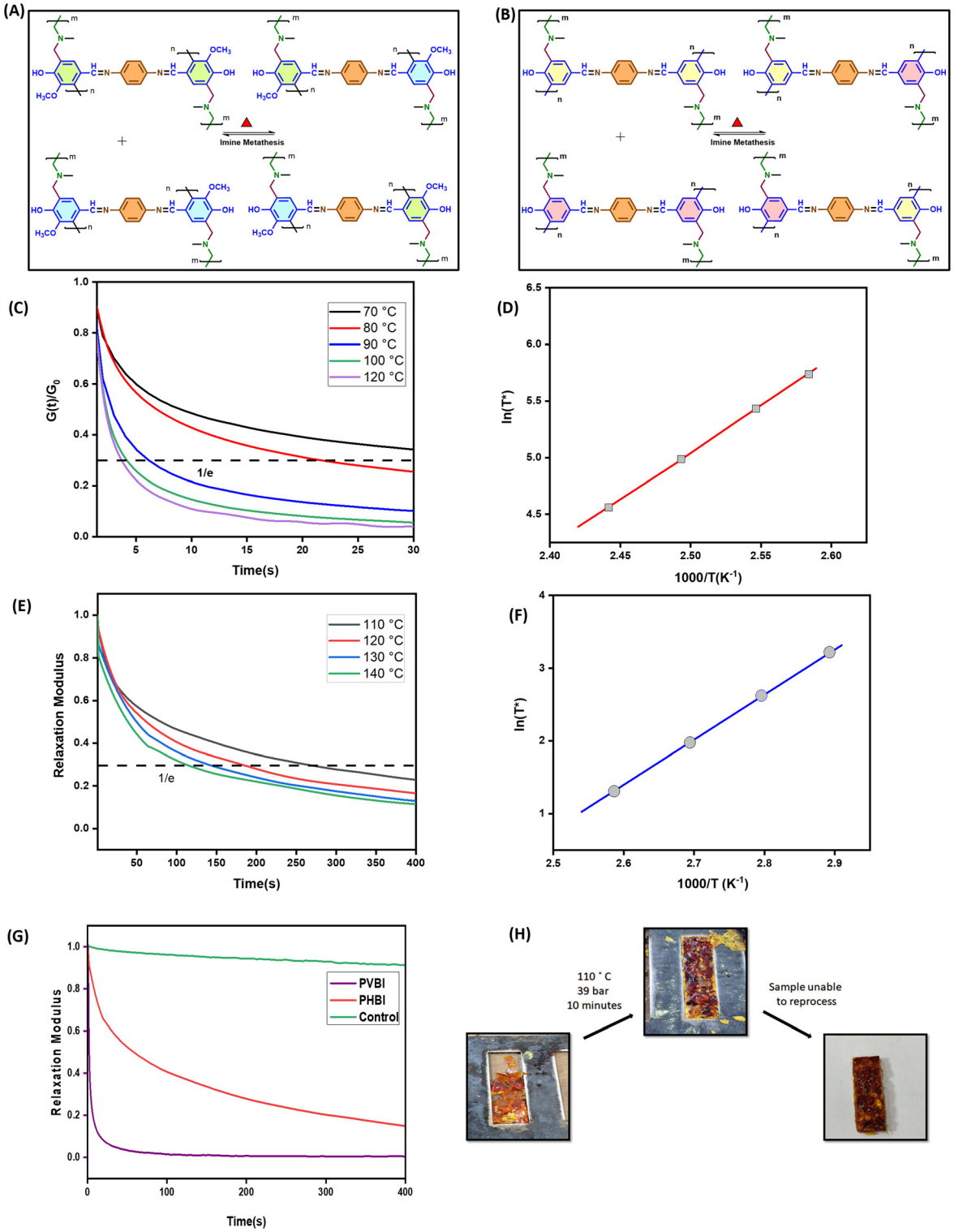

Fig. 7 (A) Imine exchange in PVBI, (B) imine exchange in PHBI, (C) normalized relaxation modulus at different temperatures *vs*. time curve for PVBI, (D) linear fitted curves from Arrhenius analysis for the calculation of activation energy for the relaxation of PVBI, (E) normalized relaxation modulus at different temperatures *vs*. time curve for PHBI, (F) linear fitted curves from Arrhenius analysis for the calculation of activation energy for the relaxation of PHBI, (G) normalized relaxation modulus at 110 °C for PVBI, PHBI and the control sample (PBASA), and (H) reprocessing studies of PBASA performed under hot pressing at 110 °C for 10 minutes.

crosslinked structure of PHBI enhances the stability of imine bonds that have been introduced. According to solvent stability testing, both PVBI and PHBI molecular networks demonstrated remarkable hydrolysis resistance and no swelling in deionized water. Water contact angle studies performed on PVBI and PHBI revealed the hydrophobic nature of the material with contact angle values of 93 ± 0.09° and 99 ± 0.17° for PVBI and PHBI, respectively (Fig. S4†).

4.6 Dynamic properties

The dynamic characteristics of PVBI and PHBI (Fig. 7(A) and (B)) were examined through stress relaxation tests. Fig. 7(C) and (E) depict the time-dependent normalized relaxation modulus $G_{(t)}/G_0$ curves within the temperature range of 70 to 120 °C for PVBI and 110 to 140 °C in the case of PHBI. Following the principles of the viscoelastic fluid model given by Maxwell, the distinctive relaxation time (τ) is defined as the period in which the ratio of $G_{(t)}$ to G_0 declines to $1/e$, which is roughly 37%. The test temperature is denoted by T, the characteristic relaxation time at infinite temperature is represented by τ_0, and the universal gas constant is denoted by R. When heated, both PVBI and PHBI display stress relaxation; this phenomenon is marked by a reduction in the relaxation time (τ) as the temperature rises. This phenomenon is in line with the distinctive characteristics of vitrimers, which are attributed to the interchange processes occurring between dynamic covalent bonds.[46,47] The Arrhenius law, given in eqn (4), can be used to derive the activation energy (E_a) for bond exchange processes.

$$\tau^*(T) = \tau_0 \exp\left(\frac{E_a}{RT}\right) \quad (4)$$

The graph shown in Fig. 7(D) and (F) displays the Arrhenius relationship, especially the natural logarithm of the relaxation time ($\ln(\tau)$) plotted against the reciprocal of temperature ($1000/T$), for two cured polybenzoxazine resins. The determined activation energy (E_a) values (Table S2†) for PVBI and PHBI amount to 51 and 68 kJ mol^{-1}, respectively. Significantly, these values are within the published range of activation energies (33–129 kJ mol^{-1}), associated with vitrimers featuring dynamic imine bonds.[41] Compared to PVBI, the PHBI resin has a greater T_g and curing reaction enthalpy, which aligns with its higher E_a. A larger E_a for imine metathesis would result from a slower exchange between imine bonds, which would trigger a higher degree of cross-linking in PHBI. These findings indicate two factors affecting the exchange kinetics of reversible bonds, which are correlated with each other. Firstly, the influence of substituent groups in the polymerization stage and, secondly, the cross-link density in the synthesized polymer have a crucial role in the speed at which exchange events occur between dynamic covalent bonds in the vitrimer.

To investigate the influence of imine linkages on the stress relaxation properties of vitrimeric polybenzoxazines, stearylamine and bisphenol-A were used as control sample (Fig. S1†). The monomer BASA was polymerized at 170 °C for 2 hours and 180 °C for 6 hours (Fig. S2†). While vitrimeric samples PVBI and PHBI exhibit relaxation at higher temperatures, the stress relaxation experiment at 110 °C reveals no correlation between temperature and relaxation for the control sample as shown in Fig. 7(G). Furthermore, under hot-pressing, PBASA could not be remolded into the desired shape, as shown in Fig. 7(H), due to the lack of dynamic imine linkages. In order to develop reprocessable polybenzoxazine networks, this work highlights the significance of reversible imine chemistry.

4.7 Recycling studies

The recycling process was done using THF, a highly polar solvent, by adding it into a glass vial containing pristine PVBI. The vial was heated at 60 °C for 2 hours, expanding polymer chains in the presence of excess THF molecules and initiating recycling with the observation of a viscous black solution containing dissolved PVBI. THF was completely removed by keeping it in a hot air oven at 100 °C for 6 hours to obtain a black powder. The PVBI powder can be turned into the desired geometry using compression molding. Therefore, the recycled

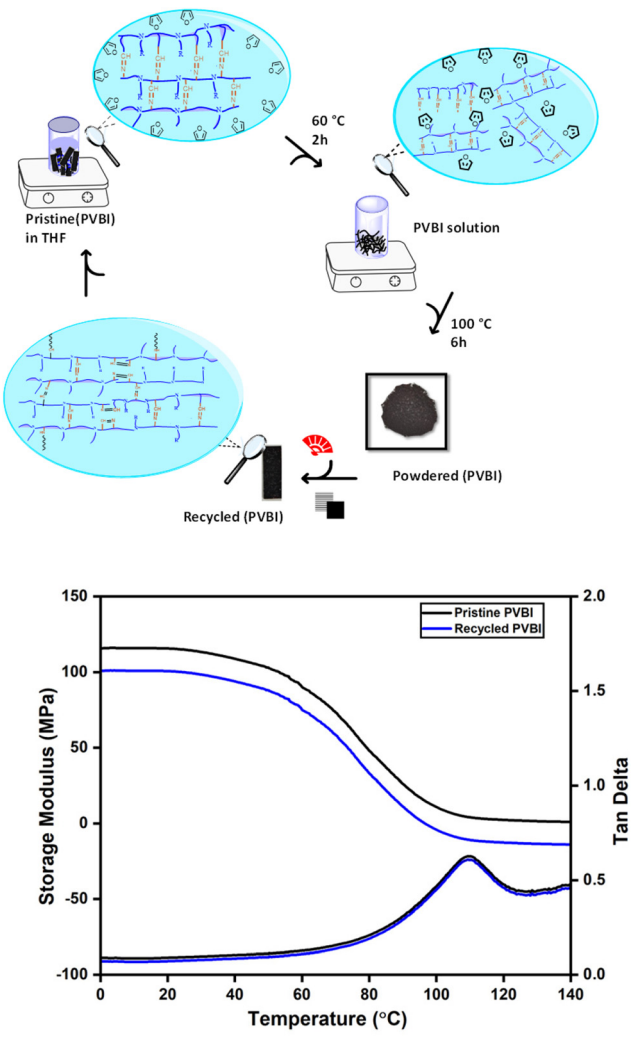

Fig. 8 Schematic of the recycling process involved in PVBI and the role of imine linkages in holding the polymer chains together.

Table 1 Performance comparisons of PVBI and PHBI with respect to a variety of test parameters

Test parameters	PVBI	PHBI
ROP activation energy	122 kJ mol^{-1}	98.9 kJ mol^{-1}
Curing conditions	100 °C–30 minutes, 170 °C–4 h, 180 °C–6 h	100 °C–30 minutes, 170 °C–4 h
$T_{5\%}$	269 °C	285 °C
Theoretical crosslink density	481 g mol^{-1}	451 g mol^{-1}
Crosslink density	414.2 mol m^{-3}	4842.2 mol m^{-3}
Storage modulus at 25 °C	115 MPa	356 MPa
T_g	107 °C	110 °C
Swelling studies	Less stable networks	More stable networks
Contact angle	93 ± 0.09°	99 ± 0.17°
Stress relaxation activation energy	51.38 kJ mol^{-1}	68.87 kJ mol^{-1}
Relaxation time at 120 °C	<4 seconds	<200 seconds
Reprocessable	Yes	Yes
Recycling studies	Using mild conditions	Using harsh conditions

PVBI powder was recovered from the rectangular steel mold upon hot-pressing. The step-by-step procedure is shown in Fig. 8. FTIR spectroscopy confirmed that the obtained recycled polymer was the same as the original PVBI, with the characteristic bands of imine, and alkyl groups appearing in the IR spectra, as shown in Fig. S5.† A DMA analysis was conducted to examine the impact of recycling on the storage modulus. Fig. 8 shows a comparative analysis of pristine and recycled PVBI, indicating the retention of 85% storage modulus for recycled PVBI with the overall impact of recycling being minimal, thereby achieving closed-loop recyclability. In the case of PHBI, recyclability under similar conditions was not possible due to the high crosslink density.

Table 1 presents a comprehensive examination of several test parameters, including the determination of activation energy for ring-opening polymerization using the Ozawa technique, stress relaxation tests, DMA analysis of both pristine and reprocessed polybenzoxazines, contact angle analysis, and recycling studies, among others. The results suggest that PHBI has significantly higher thermo-mechanical strength compared to PVBI due to a greater number of crosslinks within its polymeric network. Consequently, recycling PHBI in the presence of an excess of THF becomes challenging.

5. Conclusion

To summarise, there are two polybenzoxazines that include imine bonds, PHBI and PVBI, which were synthesized with 4-hydroxybenzaldehyde and vanillin as phenolic precursors. Steric variables play an essential role in influencing mechanical characteristics. This is attributed to distinct curing mechanisms, where chain extension occurs by either a *meta*-attack or a hydroxy attack in PVBI, while an *ortho*-attack occurs in PHBI. The crosslink density of the polybenzoxazines varied, with PHBI having a value of 4842 kJ mol^{-1} and PVBI having a value of 414 kJ mol^{-1}. This was validated in swelling investigations, which showed a greater swelling ratio for PVBI. Even after many reprocessing cycles, both polybenzoxazines retained more than 95% of their T_g content, demonstrating the reversibility of imine links that hold the polymer chain together. The *ortho*-blocked polybenzoxazines formed short chains due to the unavailability of a free *ortho*-group, as seen from the low molecular weight (M_c) between crosslinks. A lower crosslink density results in lower activation energy (E_a) for imine metathesis because segmental motions between chains containing imine bonds are more accessible to facilitate without interference from other chains. Rheological studies reveals a lower activation energy for bond relaxation in PVBI than in PHBI, with values of 51 kJ mol^{-1} and 68 kJ mol^{-1}, respectively. The use of a dynamic imine linkage gives polybenzoxazine resins with varied recyclability and reprocessability. Both polybenzoxazines with imine networks can be reprocessed using hot-pressing treatment. Even after three reprocessing cycles, the storage modulus is retained by more than 95%, and the T_g remains stable. The recycling investigations were carried out with THF, with further drying and hot-pressing toproduce recycled polybenzoxazine. This provided the system with closed-loop recyclability. PHBI having a higher crosslink density requires the use of harsh chemicals for recycling. Therefore, by tuning the crosslink density of the material, sustainable routes can be developed for vitrimeric materials.

Author contributions

Gaurav Rai: writing – original draft, conceptualization, investigation, data compilation, and methodology. Leena Nebhani: conceptualization, funding acquisition, resources, supervision, and writing – review & editing.

Data availability

The data supporting this article have been included as part of the main manuscript and ESI.†

Conflicts of interest

There are no conflicts to declare.

Acknowledgements

GR acknowledges the Research Fellowship from the Ministry of Education (MoE), Government of India. The authors thank the Central Research Facility at the Indian Institute of Technology Delhi for providing characterization facilities. LN would like to acknowledge the Science and Engineering Research Board (CRG/2022/008202).

References

1 C. J. Kloxin, T. F. Scott, B. J. Adzima and C. N. Bowman, Covalent adaptable networks (CANs): A unique paradigm in cross-linked polymers, *Macromolecules*, 2010, **43**, 2643–2653, DOI: **10.1021/ma902596s**.

2 J. M. Winne, L. Leibler and F. E. Du Prez, Dynamic covalent chemistry in polymer networks: A mechanistic perspective, *Polym. Chem.*, 2019, **10**, 6091–6108, DOI: **10.1039/c9py01260e**.

3 L. Yue, V. S. Bonab, D. Yuan, A. Patel, V. Karimkhani and I. Manas-Zloczower, Vitrimerization: A Novel Concept to Reprocess and Recycle Thermoset Waste via Dynamic Chemistry, *Global Challenges*, 2019, **3**, 1800076, DOI: **10.1002/gch2.201800076**.

4 N. J. Van Zee and R. Nicolaÿ, Vitrimers: Permanently crosslinked polymers with dynamic network topology, *Prog. Polym. Sci.*, 2020, **104**, 101233, DOI: **10.1016/j.progpolymsci.2020.101233**.

5 B. Krishnakumar, R. V. S. P. Sanka, W. H. Binder, V. Parthasarthy, S. Rana and N. Karak, Vitrimers: Associative dynamic covalent adaptive networks in thermoset polymers, *Chem. Eng. J.*, 2020, **385**, 123820, DOI: **10.1016/j.cej.2019.123820**.

6 M. Podgórski, B. D. Fairbanks, B. E. Kirkpatrick, M. McBride, A. Martinez, A. Dobson, N. J. Bongiardina and C. N. Bowman, Toward Stimuli-Responsive Dynamic Thermosets through Continuous Development and Improvements in Covalent Adaptable Networks (CANs), *Adv. Mater.*, 2020, **32**, 1906876, DOI: **10.1002/adma.201906876**.

7 C. J. Kloxin and C. N. Bowman, Covalent adaptable networks: Smart, reconfigurable and responsive network systems, *Chem. Soc. Rev.*, 2013, **42**, 7161–7173, DOI: **10.1039/c3cs60046g**.

8 A. Jourdain, R. Asbai, O. Anaya, M. M. Chehimi, E. Drockenmuller and D. Montarnal, Rheological Properties of Covalent Adaptable Networks with 1,2,3-Triazolium Cross-Links: The Missing Link between Vitrimers and Dissociative Networks, *Macromolecules*, 2020, **53**, 1884–1900, DOI: **10.1021/acs.macromol.9b02204**.

9 B. R. Elling and W. R. Dichtel, Reprocessable Cross-Linked Polymer Networks: Are Associative Exchange Mechanisms Desirable?, *ACS Cent. Sci.*, 2020, **6**, 1488–1496, DOI: **10.1021/acscentsci.0c00567**.

10 G. M. Scheutz, J. J. Lessard, M. B. Sims and B. S. Sumerlin, Adaptable Crosslinks in Polymeric Materials: Resolving the Intersection of Thermoplastics and Thermosets, *J. Am. Chem. Soc.*, 2019, **141**, 16181–16196, DOI: **10.1021/jacs.9b07922**.

11 N. Zheng, Y. Xu, Q. Zhao and T. Xie, Dynamic Covalent Polymer Networks: A Molecular Platform for Designing Functions beyond Chemical Recycling and Self-Healing, *Chem. Rev.*, 2021, **121**, 1716–1745, DOI: **10.1021/acs.chemrev.0c00938**.

12 V. Schenk, K. Labastie, M. Destarac, P. Olivier and M. Guerre, Vitrimer composites: current status and future challenges, *Mater. Adv.*, 2022, **3**, 8012–8029, DOI: **10.1039/d2ma00654e**.

13 Z. Zhu, S. West, H. Chen, G. H. Lai, S. Uenuma, K. Ito, M. Kotaki and H. J. Sue, Mechanically Interlocked Vitrimer Based on Polybenzoxazine and Polyrotaxane, *ACS Appl. Polym. Mater.*, 2023, **5**, 3971–3978, DOI: **10.1021/acsapm.3c00196**.

14 J. Chen, X. Lu and Z. Xin, A bio-based reprocessable and degradable polybenzoxazine with acetal structures, *React. Funct. Polym.*, 2023, **191**, 105653, DOI: **10.1016/j.reactfunctpolym.2023.105653**.

15 Z. Wen, L. Bonnaud, P. Dubois and J. M. Raquez, Catalyst-free reprocessable crosslinked biobased polybenzoxazine-polyurethane based on dynamic carbamate chemistry, *J. Appl. Polym. Sci.*, 2022, **139**, 52120, DOI: **10.1002/app.52120**.

16 S. Gulyuz, Y. Yagci and B. Kiskan, Exploiting the reversible covalent bonding of boronic acids for self-healing/recycling of main-chain polybenzoxazines, *Polym. Chem.*, 2022, **13**, 3631–3638, DOI: **10.1039/d2py00068g**.

17 M. Ciaccia and S. Di Stefano, Mechanisms of imine exchange reactions in organic solvents, *Org. Biomol. Chem.*, 2015, **13**, 646–654, DOI: **10.1039/c4ob02110j**.

18 R. W. Layer, *Chem. Rev.*, 1963, **63**(5), 489–510, DOI: **10.1021/cr60225a003**.

19 X. Shen, Y. Ma, S. Luo, R. Tao, D. An, X. Wei, Y. Jin, L. Qiu and W. Zhang, Malleable and recyclable imide-imine hybrid thermosets: Influence of imide structure on material property, *Mater. Adv.*, 2021, **2**, 4333–4338, DOI: **10.1039/d1ma00311a**.

20 S. K. Schoustra, J. A. Dijksman, H. Zuilhof and M. M. J. Smulders, Molecular control over vitrimer-like mechanics-tuneable dynamic motifs based on the Hammett equation in polyimine materials, *Chem. Sci.*, 2021, **12**, 293–302, DOI: **10.1039/d0sc05458e**.

21 S. K. Schoustra, T. Groeneveld and M. M. J. Smulders, The effect of polarity on the molecular exchange dynamics in imine-based covalent adaptable networks, *Polym. Chem.*, 2021, **12**, 1635–1642, DOI: **10.1039/d0py01555e**.

22 P. Taynton, H. Ni, C. Zhu, K. Yu, S. Loob, Y. Jin, H. J. Qi and W. Zhang, Repairable woven carbon fiber composites with full recyclability enabled by malleable polyimine networks, *Adv. Mater.*, 2016, **28**, 2904–2909, DOI: **10.1002/adma.201505245**.

23 Y. Yang, L. Huang, R. Wu, W. Fan, Q. Dai, J. He and C. Bai, Assembling of Reprocessable Polybutadiene-Based Vitrimers

with High Strength and Shape Memory via Catalyst-Free Imine-Coordinated Boroxine, *ACS Appl. Mater. Interfaces*, 2020, **12**, 33305–33314, DOI: 10.1021/acsami.0c09712.

24 P. R. Christensen, A. M. Scheuermann, K. E. Loeffler and B. A. Helms, Closed-loop recycling of plastics enabled by dynamic covalent diketoenamine bonds, *Nat. Chem.*, 2019, **11**, 442–448, DOI: 10.1038/s41557-019-0249-2.

25 K. Hong, Q. Sun, X. Zhang, L. Fan, T. Wu, J. Du and Y. Zhu, Fully Bio-Based High-Performance Thermosets with Closed-Loop Recyclability, *ACS Sustainable Chem. Eng.*, 2022, **10**, 1036–1046, DOI: 10.1021/acssuschemeng.1c07523.

26 M. A. Lucherelli, A. Duval and L. Avérous, Biobased vitrimers: Towards sustainable and adaptable performing polymer materials, *Prog. Polym. Sci.*, 2022, **127**, 101515, DOI: 10.1016/j.progpolymsci.2022.101515.

27 N. De, A. Watuthanthrige, P. Chakma and D. Konkolewicz, *Designing Dynamic Materials from Dynamic bonds to Macromolecular Architecture*, 2020.

28 P. Taynton, K. Yu, R. K. Shoemaker, Y. Jin, H. J. Qi and W. Zhang, Heat- or water-driven malleability in a highly recyclable covalent network polymer, *Adv. Mater.*, 2014, **26**, 3938–3942, DOI: 10.1002/adma.201400317.

29 M. Guerre, C. Taplan, J. M. Winne and F. E. Du Prez, Vitrimers: directing chemical reactivity to control material properties, *Chem. Sci.*, 2020, **11**, 4855–4870, DOI: 10.1039/d0sc01069c.

30 L. Li, X. Chen, K. Jin and J. M. Torkelson, Vitrimers Designed Both to Strongly Suppress Creep and to Recover Original Cross-Link Density after Reprocessing: Quantitative Theory and Experiments, *Macromolecules*, 2018, **51**, 5537–5546, DOI: 10.1021/acs.macromol.8b00922.

31 W. Denissen, M. Droesbeke, R. Nicola, L. Leibler, J. M. Winne and F. E. Du Prez, Chemical control of the viscoelastic properties of vinylogous urethane vitrimers, *Nat. Commun.*, 2017, **8**, 14857, DOI: 10.1038/ncomms14857.

32 X. Lei, Y. Jin, H. Sun and W. Zhang, Rehealable imide-imine hybrid polymers with full recyclability, *J. Mater. Chem. A*, 2017, **5**, 21140–21145, DOI: 10.1039/c7ta07076d.

33 M. Zhen, H. Zhen, X. Zuo, Z. Wu, Z. Li, Y. Liu and M. Run, Synthesis, ring-opening polymerization, and properties of benzoxazines based on o- and p-hydroxybenzyl alcohols, *High Perform. Polym.*, 2023, **35**, 91–102, DOI: 10.1177/09540083221113974.

34 L. Zhang, Z. Zhao, Z. Dai, L. Xu, F. Fu, T. Endo and X. Liu, Unexpected Healability of an ortho-Blocked Polybenzoxazine Resin, *ACS Macro Lett.*, 2019, **8**, 506–511, DOI: 10.1021/acsmacrolett.9b00083.

35 C. Aydogan, B. Kiskan, S. O. Hacioglu, L. Toppare and Y. Yagci, Electrochemical manipulation of adhesion strength of polybenzoxazines on metal surfaces: From strong adhesion to dismantling, *RSC Adv.*, 2014, **4**, 27545–27551, DOI: 10.1039/c4ra03763d.

36 A. Van, K. Chiou and H. Ishida, Use of renewable resource vanillin for the preparation of benzoxazine resin and reactive monomeric surfactant containing oxazine ring, *Polymer*, 2014, **55**, 1443–1451, DOI: 10.1016/j.polymer.2014.01.041.

37 L. Han, D. Iguchi, P. Gil, T. R. Heyl, V. M. Sedwick, C. R. Arza, S. Ohashi, D. J. Lacks and H. Ishida, Oxazine Ring-Related Vibrational Modes of Benzoxazine Monomers Using Fully Aromatically Substituted, Deuterated, 15N Isotope Exchanged, and Oxazine-Ring-Substituted Compounds and Theoretical Calculations, *J. Phys. Chem. A*, 2017, **121**, 6269–6282, DOI: 10.1021/acs.jpca.7b05249.

38 X.-L. Zhao, Y.-D. Li, Y. Weng and J.-B. Zeng, Biobased epoxy covalent adaptable networks for high-performance recoverable adhesives, *Industrial Crops & Products*, 2023, **192**, 116016, DOI: 10.1016/j.indcrop.2022.116016.

39 S. Zhao and M. M. Abu-Omar, Recyclable and Malleable Epoxy Thermoset Bearing Aromatic Imine Bonds, *Macromolecules*, 2018, **51**, 9816–9824, DOI: 10.1021/acs.macromol.8b01976.

40 Y. Bai, P. Yang, Y. Song, R. Zhu and Y. Gu, Effect of hydrogen bonds on the polymerization of benzoxazines: Influence and control, *RSC Adv.*, 2016, **6**, 45630–45635, DOI: 10.1039/c6ra08881c.

41 N. Tratnik, N. R. Tanguy and N. Yan, Recyclable, self-strengthening starch-based epoxy vitrimer facilitated by exchangeable disulfide bonds, *Chem. Eng. J.*, 2023, **451**, 138610, DOI: 10.1016/j.cej.2022.138610.

42 A. Adjaoud, L. Puchot and P. Verge, High-Tgand Degradable Isosorbide-Based Polybenzoxazine Vitrimer, *ACS Sustainable Chem. Eng.*, 2022, **10**, 594–602, DOI: 10.1021/acssuschemeng.1c07093.

43 P. Chakma and D. Konkolewicz, Dynamic Covalent Bonds in Polymeric Materials, *Angew. Chem.*, 2019, **131**, 9784–9797, DOI: 10.1002/ange.201813525.

44 H. Liu, Q. Q. Liu, L. Tian, L. Y. Wang, K. Xu, Q. X. Chen and B. L. Ou, Structural effects of highly π-conjugated mesogenic Schiff-base moiety on the cationic polymerization of benzoxazine and formation of ordered morphologies, *React. Funct. Polym.*, 2018, **124**, 139–148, DOI: 10.1016/j.reactfunctpolym.2018.01.015.

45 X. Liu, E. Zhang, Z. Feng, J. Liu, B. Chen and L. Liang, Degradable bio-based epoxy vitrimers based on imine chemistry and their application in recyclable carbon fiber composites, *J. Mater. Sci.*, 2021, **56**, 15733–15751, DOI: 10.1007/s10853-021-06291-5.

46 S. P. O. Danielsen, H. K. Beech, S. Wang, B. M. El-Zaatari, X. Wang, L. Sapir, T. Ouchi, Z. Wang, P. N. Johnson, Y. Hu, D. J. Lundberg, G. Stoychev, S. L. Craig, J. A. Johnson, J. A. Kalow, B. D. Olsen and M. Rubinstein, Molecular Characterization of Polymer Networks, *Chem. Rev.*, 2021, **121**, 5042–5092, DOI: 10.1021/acs.chemrev.0c01304.

47 C. W. H. Rajawasam, O. J. Dodo, M. A. S. N. Weerasinghe, I. O. Raji, S. V. Wanasinghe, D. Konkolewicz and N. De Alwis Watuthanthrige, Educational series: characterizing crosslinked polymer networks, *Polym. Chem.*, 2023, **15**, 219–247, DOI: 10.1039/d3py00914a.

